JCI insight

Critical role of Interleukin 21 and T follicular helper cells in hypertension and vascular dysfunction

Bethany L. Dale, … , Holly M. Scott Algood, Meena S. Madhur

JCI Insight. 2019. https://doi.org/10.1172/jci.insight.129278.

Research In-Press Preview **Cardiology** **Immunology**

T and B cells have been implicated in hypertension, but the mechanisms by which they produce a coordinated response is unknown. T follicular helper (Tfh) cells that produce interleukin 21 (IL21) promote germinal center (GC) B cell responses leading to immunoglobulin (Ig) production. Here we investigate the role of IL21 and Tfh cells in hypertension. In response to angiotensin (Ang) II-induced hypertension, T cell IL21 production is increased, and *Il21*$^{-/-}$ mice develop blunted hypertension, attenuated vascular end-organ damage, and decreased interleukin 17A (IL17A) and interferon gamma production. Tfh-like cells and GC B cells accumulate in the aorta and plasma IgG1 is increased in hypertensive WT but not *Il21*$^{-/-}$mice. Furthermore, Tfh cell deficient mice develop blunted hypertension and vascular hypertrophy in response to Ang II infusion. Importantly, IL21 neutralization reduces blood pressure (BP) and reverses endothelial dysfunction and vascular inflammation. Moreover, recombinant IL21 impairs endothelium-dependent relaxation ex vivo and decreases nitric oxide production from cultured endothelial cells. Finally, we show in humans that peripheral blood T cell production of IL21 correlates with systolic BP and IL17A production. These data suggest that IL21 may be a novel therapeutic target for the treatment of hypertension and its micro- and macrovascular complications.

CRITICAL ROLE OF INTERLEUKIN 21 AND T FOLLICULAR HELPER CELLS IN HYPERTENSION AND VASCULAR DYSFUNCTION

Dale
IL21 and Tfh cells in hypertension

Bethany L. Dale[1], Arvind K. Pandey[2*], Yuhan Chen[3], Charles D. Smart[1], Fanny Laroumanie[3], Mingfang Ao[3], Liang Xiao[3], Anna E. Dikalova[3], Sergey I. Dikalov[3], Fernando Elijovich[3], Jason D. Foss[3], Natalia R. Barbaro[3], Justin P. Van Beusecum[3], Serpil M. Deger[4], Aseel Alsouqi[4], Hana A. Itani[3**], Allison E. Norlander[1***], Matthew R. Alexander[2], Shilin Zhao[5], T. Alp Ikizler[4], Holly M. Scott Algood[6,7,8], Meena S. Madhur[1,2,3,7]

[1]Department of Molecular Physiology and Biophysics, Vanderbilt University, Nashville, TN, USA; [2]Department of Medicine, Division of Cardiovascular Medicine, Vanderbilt University Medical Center (VUMC), Nashville, TN, USA; [3]Department of Medicine, Division of Clinical Pharmacology, VUMC, Nashville, TN,USA; [4]Department of Medicine, Division of Nephrology, VUMC, Nashville, TN, USA; [5]Department of Biostatistics, VUMC, Nashville, TN, USA; [6]Department of Medicine, Division of Infectious Disease, VUMC, Nashville, TN, USA; [7]Vanderbilt Institute for Infection, Immunology, and Inflammation, Nashville, TN, USA; [8]Vanderbilt Digestive Diseases Research Center, Nashville, TN, USA

Present affiliations: *Division of Cardiovascular Medicine, Brigham and Women's Hospital, Harvard Medical School, Boston, MA, USA; **Department of Pharmacology and Toxicology, American University of Beirut, Beirut, Lebanon; ***Division of Allergy, Pulmonary, and Critical Care, VUMC, Nashville, TN, USA

Address for Correspondence:
Meena S. Madhur, MD, PhD
Department of Medicine, Division of Clinical Pharmacology
2215 Garland Avenue, P415D MRB IV
Vanderbilt University
Nashville, TN 37232
615-875-3273
meena.madhur@vanderbilt.edu

TAI is a consultant for Fresenius Kabi, Corvidia, and Nestle and MSM holds a patent on monocyte biomarkers for hypertension (PCT/US2018/029482).

ABSTRACT

T and B cells have been implicated in hypertension, but the mechanisms by which they produce a coordinated response is unknown. T follicular helper (Tfh) cells that produce interleukin 21 (IL21) promote germinal center (GC) B cell responses leading to immunoglobulin (Ig) production. Here we investigate the role of IL21 and Tfh cells in hypertension. In response to angiotensin (Ang) II-induced hypertension, T cell IL21 production is increased, and *Il21*$^{-/-}$ mice develop blunted hypertension, attenuated vascular end-organ damage, and decreased interleukin 17A (IL17A) and interferon gamma production. Tfh-like cells and GC B cells accumulate in the aorta and plasma IgG1 is increased in hypertensive WT but not *Il21*$^{-/-}$ mice. Furthermore, Tfh cell deficient mice develop blunted hypertension and vascular hypertrophy in response to Ang II infusion. Importantly, IL21 neutralization reduces blood pressure (BP) and reverses endothelial dysfunction and vascular inflammation. Moreover, recombinant IL21 impairs endothelium-dependent relaxation ex vivo and decreases nitric oxide production from cultured endothelial cells. Finally, we show in humans that peripheral blood T cell production of IL21 correlates with systolic BP and IL17A production. These data suggest that IL21 may be a novel therapeutic target for the treatment of hypertension and its micro- and macrovascular complications.

INTRODUCTION

Hypertension affects nearly one-half of all adults in the United States (1). As a key contributor to vascular disease, chronic kidney disease, and heart failure, hypertension is the leading risk factor for global mortality (2). Unfortunately, nearly 50% of people with hypertension have uncontrolled blood pressures despite current pharmacological therapies, highlighting the need for a better understanding of the pathophysiology of this disease and identification of novel therapeutic targets (3).

A potential role for immune cells and elevated serum immunoglobulins in hypertension was noted over 50 years ago (4, 5), but we are still far from understanding the key immune cell subsets and pathways that lead to hypertension and hypertensive end-organ damage. In 2007, Guzik et al. demonstrated that mice deficient in T and B cells develop blunted Ang II-induced hypertension, with the hypertensive response restored by adoptive transfer of T cells (6). Our group and others demonstrated pathogenic effects of specific T cell subsets, most notably interleukin 17A (IL17A) producing Th17 cells and interferon gamma (IFNγ) producing Th1/Tc1 cells, and protective effects of T regulatory (Treg) cells in hypertension (7). IL17A and IFNγ induce vascular dysfunction, glomerular injury, and renal salt and water reabsorption (7, 8). In 2015, Chan et al. demonstrated that pharmacological or genetic depletion of B cells protects against experimental hypertension (9). The specific T helper subset that provides help to B cells is T follicular helper (Tfh) cells that produce IL21, and yet the role of IL21 and Tfh cells in hypertension is unknown. Importantly, in addition to promoting Th17 and Th1 cells, IL21 from Tfh cells drives a germinal center (GC) reaction in secondary or tertiary lymphoid organs resulting in GC B cell immunoglobulin (Ig) class switching (e.g. IgM $\rightarrow$ IgG) and high affinity antibody production (10-13). Whether hypertension is associated with a germinal center response is not known.

Here we report the novel finding that hypertension is associated with increased Tfh and GC B cells in the aorta and increased GC B cells in secondary lymphoid organs along with increased plasma IgG1. Using genetic and/or pharmacological inhibition of IL21 and Tfh cells, we demonstrate a previously undefined role for IL21 in hypertension pathogenesis and vascular dysfunction, suggesting that IL21 and Tfh cells may serve as novel therapeutic targets for this disease.

RESULTS

Hypertension is associated with increased CD4$^+$ T cell production of IL21, and IL21 deficiency attenuates the rise in blood pressure (BP) in response to hypertensive stimuli. To determine the role of IL21 in hypertension, we first isolated splenic CD4$^+$ T cells from C57Bl/6J wild type (WT) mice infused with vehicle or Ang II for 4 weeks and cultured them in the presence of anti-CD3 and anti-CD28 antibodies for 72 hrs. We found that CD4$^+$ T cells from hypertensive mice display increased *Il21* mRNA expression (**Figure 1A**) and increased IL21 secretion (**Figure 1B**). We then investigated the effect of IL21 deficiency on Ang-II induced hypertension. Following 4 weeks of Ang II (490 ng/kg/min) infusion, *Il21*$^{-/-}$ male mice develop a systolic BP approximately 20 mmHg lower than WT animals by tail cuff (**Figure 1C**) and invasive radio telemetry (**Figure 1D**). Diastolic BP was similarly reduced in *Il21*$^{-/-}$ mice compared to WT controls with no change in heart rate (**Figures 1E and 1F**). To determine if there are gender differences in the effect of IL21 on hypertension, we studied female mice and found that both the hypertensive response and effect of IL21 deficiency were similar to those observed in male mice (**Figure S1A**). To confirm that the BP protection was not unique to the Ang II model, we investigated the effect of IL21 deficiency in a salt-sensitive hypertension model characterized by uninephrectomy, implantation of a deoxycorticosterone acetate (DOCA) pellet, and 1% NaCl in the drinking water and observed a similar 20 mmHg reduction in systolic BP (**Figure S1B**). All further studies were conducted in male mice using the Ang II hypertension model.

Loss of IL21 protects against Ang II-induced vascular remodeling and endothelial dysfunction. Hypertension is associated with increased aortic collagen deposition, vascular smooth muscle cell hypertrophy, and microvascular endothelial dysfunction. To determine the effect of IL21 deficiency on vascular remodeling and endothelial function, WT and *Il21*$^{-/-}$ mice were infused with vehicle or Ang II for 4 weeks. Importantly, *Il21*$^{-/-}$ mice thoracic aortas exhibit significantly less aortic collagen deposition and reduced medial hypertrophy (**Figures 2A-C**). Representative aortic

cross-sections are shown in **Figures 2A-B** with quantification in **Figure 2C**. Resistance artery endothelial function was assessed by measuring endothelium-dependent and -independent relaxation of third-order mesenteric arterioles. A modest baseline impairment in endothelium-dependent relaxation to acetylcholine (Ach) is present in *Il21*$^{-/-}$ mesenteric arterioles, but the key finding is that the *Il21*$^{-/-}$ mice are completely protected from further endothelial dysfunction in response to Ang II infusion, while WT vessels exhibit a severe impairment in endothelium-dependent relaxation in response to Ang II. There was no effect of Ang II or IL21 deficiency on endothelium-independent relaxation to sodium nitroprusside (SNP) (**Figure 2D**). Since vascular reactivity can be mediated by alterations in superoxide levels, we measured superoxide production in isolated mesenteric arterioles. Interestingly, *Il21*$^{-/-}$ mice exhibit increased superoxide levels at baseline, consistent with their baseline impairment in vascular reactivity, but no further increase in response to Ang II infusion. In contrast, WT mice exhibit a marked upregulation of superoxide production in response to Ang II-induced hypertension (**Figure 2E**).

IL21 deficiency blunts early vascular infiltration of natural killer (NK) T cells and macrophages. We previously showed that during the initial phase of Ang II-induced hypertension (day 7), there is an increase in total aortic leukocytes composed primarily of innate immune cells such as F4/80^{+} monocytes/macrophages (14). Here we quantified total leukocytes (CD45^{+}), NK T cells (CD3^{+}NK1.1^{+}), macrophages (F4/80^{+}Ly6G^{-}), and neutrophils (F4/80^{-}Ly6G^{+}) in the aorta of WT and *Il21*$^{-/-}$ mice following 7 days of vehicle or Ang II infusion. Flow cytometry gating strategy and fluorescence minus one controls are shown in **Figure S2**. Macrophages and neutrophils were gated from CD11b^{+} cells and NK T cells were gated from CD3^{+} cells (**Figure S2**). Representative biaxial flow cytometry dot plots are shown for each group (**Figure 3A**). We found that Ang II-induced hypertension is associated with an early increase in total leukocytes, NK T cells, and macrophages, and this increase is abrogated in *Il21*$^{-/-}$ mice (**Figure 3B**). Neutrophils were not

increased by Ang II infusion or affected by IL21 deficiency (**Figure 3B**). Thus, IL21 deficiency protects from early innate immune cell infiltration into the aorta.

Hypertension induces GC-like cells in the vasculature and increased splenic T cell cytokine production in an IL21 dependent manner. Peripheral GC-like cells have been found in inflamed tissues in autoimmune conditions such as multiple sclerosis, rheumatoid arthritis, and lupus nephritis (15-17). Since IL21 is a key driver of the GC reaction and produced predominantly by Tfh or peripheral helper T (Tph) cells (which do not express the lymphoid follicle homing chemokine receptor CXCR5 but still retain PD1) (16), we determined whether the number of these cells and GC B cells are altered in the aorta during experimental hypertension. WT and *Il21*$^{-/-}$ mice were infused with vehicle or Ang II for 4 weeks. Flow cytometry gating strategy and fluorescence minus one controls are shown in **Figures S3-S4**. Total leukocytes, CD4^{+} T cells, and CD19^{+}B220^{+} B cells increase in WT mice in response to 4 weeks of Ang II infusion, and this increase is blunted in *Il21*$^{-/-}$ mice (**Figures S3-S4**). Tfh cells and Tph cells are gated from CD4^{+} T cells, and GC B cells are gated from total B cells that are also IgD^{-} and CD138^{-}. Representative biaxial flow cytometry dot plots for Tph cells (PD1^{+}CXCR5^{-}), Tfh cells (PD1^{+}CXCR5^{+}), and GC B cells (Fas^{+}GL7^{+}) are shown for each group (**Figures 4A-B**). We found that Tph, Tfh, and GC B cells accumulate in the aorta of WT, but not *Il21*$^{-/-}$ animals, in response to Ang II-induced hypertension (**Figure 4C**). We previously showed that hypertension is associated with increased T cell production of the pro-inflammatory cytokines IL17A and IFNγ (18, 19). IL21 can potentially modulate the balance of Th17, Th1, and Treg subsets in disease (11, 20). Therefore, we investigated the effect of IL21 deficiency on T cell production of IL17A, IFNγ, and IL10 in hypertension. Consistent with our prior results, we detected an increase in CD4^{+} T cell production of IL17A and CD8^{+} T cell production of IFNγ in splenic T cells cultured from hypertensive vs normotensive mice, and these hypertension-induced changes were completely abrogated in *Il21*$^{-/-}$ mice. Neither Ang II nor IL21 deficiency affected CD4^{+} T cell production of IL10 (**Figure 4D**).

Thus, hypertension is associated with increased aortic accumulation of Tph, Tfh, and GC B cells and increased splenic T cell production of IL17A and IFNγ in an IL21 dependent manner.

Hypertension induces an IL21 dependent GC response, tertiary lymphoid development, and increased IgG production. The primary effector function of Tfh cells is to stimulate GC B cells in secondary and tertiary lymphoid organs to undergo cycles of proliferation and selection leading to the production of class switched and/or high affinity antibodies and long-lived plasma cells (21). Although B cells have recently been implicated in the pathogenesis of hypertension (9), it is not known whether hypertension is associated with a GC reaction as observed in the setting of infection, vaccination, and some autoimmune diseases (22). Due to their proximity to mesenteric resistance vessels in which IL21 deficiency was shown to play a protective role, we isolated mesenteric lymph nodes from WT and *Il21*$^{-/-}$ mice infused with vehicle or Ang II for 4 weeks and quantified Tfh and GC B cells. Tfh cells were expressed as percent of total CD4^{+} T cells, and GC B cells were expressed as percent of total B cells. Ang II infusion did not alter the percentage of Tfh cells in mesenteric lymph nodes of WT mice, but Tfh cells were reduced both at baseline (vehicle infusion) and after Ang II infusion in *Il21*$^{-/-}$ mice (**Figure 5A**). Interestingly, the percentage of GC B cells increased in mesenteric lymph nodes of WT mice in response to Ang II-induced hypertension. In contrast, *Il21*$^{-/-}$ mice had fewer GC B cells at baseline (vehicle infusion) and exhibited no increase in these cells after Ang II infusion (**Figure 5B**). Of note, neither hypertension nor IL21 deficiency is associated with changes in overall immune cell numbers or composition in the mesenteric lymph nodes as total CD45^{+} leukocytes, percent of CD4^{+} T cells, and percent of total B cells were unchanged in all four groups (**Figure S5A**). We then investigated follicular architecture and germinal centers in the spleens of WT and *Il21*$^{-/-}$ mice following 4 weeks of vehicle or Ang II infusion. Interestingly, and consistent with the findings of Drummond and colleagues (9), we observed an increase in follicle number and decrease in follicle size in spleens of hypertensive WT mice, and this finding was attenuated in *Il21*$^{-/-}$ mice. Furthermore, PNA

staining, which detects GC B cells, is weaker in *Il21*$^{-/-}$ spleens (**Figure 5C**) consistent with the findings of Linterman et al. (12). To determine whether tertiary lymphoid organs (TLOs) form in hypertensive aortas, we performed whole mount immunohistochemistry of aortas from WT mice infused with 4 weeks of Ang II. We found evidence of T and B cell clusters resembling TLOs as well as sites of unstructured T and B cell aggregates (**Figure 5D**) in hypertensive aortas. We then quantified plasma immunoglobulins in WT and *Il21*$^{-/-}$ mice infused with 4 weeks of vehicle or Ang II. Ang II-induced hypertension is associated with an increase in total IgG, driven primarily by the IgG1 subclass, in WT but not *Il21*$^{-/-}$ mice. IgG2a was not significantly increased by Ang II infusion but was higher in Ang II-infused WT vs *Il21*$^{-/-}$ mice. There was no change in the other IgG subclasses or IgM between all four groups (**Figures 5E and S5B**). Taken together, these data suggest that hypertension is associated with an IL21-dependent germinal center response.

Hypertensive DCs induce Tfh cell polarization, and Tfh cells play a critical role in hypertension. Hypertensive stimuli have been shown to activate DCs which in turn stimulate T cell proliferation through presentation of isolevuglandin-modified peptides (23). To determine if hypertensive DCs promote naïve T cells to polarize to Tfh cells, we utilized a co-culture assay. Splenic DCs from mice infused with vehicle or Ang II for 2 weeks were isolated and co-cultured with naïve CD4^{+} T cells at a 1:5 ratio for 72 hours (**Figure 6A**). Hypertensive DCs induced a 2-fold increase in Tfh cell polarization compared to normotensive DCs (**Figure 6A**). Since BCL6 is an essential transcription factor for the Tfh cell differentiation program, we generated mice with Tfh cell deficiency by crossing floxed BCL6 mice (*Bcl6*$^{fl/fl}$) with mice transgenic for cre recombinase under the control of the CD4 promoter (*Tg*^{CD4cre}). To confirm T cell deletion of BCL6, we isolated CD4^{+} T cells from the spleen of *Bcl6*$^{fl/fl}$ *Tg*^{CD4cre} mice and cre negative *Bcl6*$^{fl/fl}$ littermate controls and demonstrated a significant reduction in *Bcl6* expression by qRT-PCR in *Bcl6*$^{fl/fl}$*Tg*^{CD4cre} mice (**Figure S6A**). To determine the effect of Tfh cell depletion on hypertension, we infused Ang II for 4 weeks in *Bcl6*$^{fl/fl}$*Tg*^{CD4cre} mice and *Bcl6*$^{fl/fl}$ littermate controls. Although the initial rise in systolic

BP was similar in both groups of mice, Tfh deficient mice were unable to sustain the hypertensive response, reaching a systolic BP approximately 20 mmHg lower than floxed control mice by day 28 (**Figure 6B**). We then assessed aortic smooth muscle cell hypertrophy, mesenteric endothelial function, and vascular inflammation in these mice. Aortic media thickness was significantly decreased in the Tfh cell deficient mice following Ang II infusion with no change in endothelium-dependent relaxation (**Figures 6C-D and S6B**), similar to that seen in IL21 deficient mice. In contrast to *Il21*$^{-/-}$ mice, there was no change in the overall number of aortic total leukocytes, CD4+ T cells, B cells, and Tph cells, but there was a specific reduction in aortic Tfh and GC B cells (**Figure 6E**). This intermediate phenotype observed in Tfh deficient mice compared to IL21 deficient mice suggests that there may be additional sources of IL21, such as Tph cells, that are relevant in hypertension or a compensatory increase in other T cell subsets, such as Th17 cells. Indeed, we isolated splenic T cells and quantified IFNγ and IL17A production from Tfh deficient and floxed control mice following 4 weeks of Ang II infusion and found no change in IFNγ production, but increased IL17A production (**Figure S6C**). Taken together, these results highlight the critical role played by Tfh cells in hypertension independent of alterations in other T cell subsets.

Anti-IL21 treatment lowers blood pressure and reverses endothelial dysfunction and vascular inflammation. To determine whether pharmacologic targeting of IL21 may be a beneficial therapeutic strategy, WT mice were infused with Ang II for 4 weeks and randomized to receive twice weekly injections of isotype control or an anti-IL21 neutralizing antibody (100μg/injection) during the last 2 weeks. Mice that received anti-IL21 treatment exhibit an approximately 15 mmHg reduction in BP (**Figure 7A**). Importantly, anti-IL21 treatment restores endothelium-dependent relaxation to Ach to levels comparable with vehicle infused WT animals (**Figure 7B**). Endothelium-independent relaxation to SNP was similar in both groups (**Figure S7**). In addition, anti-IL21 treatment decreases aortic inflammatory cells, including Tph, Tfh, and GC B cells, to levels

comparable to vehicle infused WT animals (**Figure 7E**). Thus, inhibition of IL21 lowers BP and reverses endothelial dysfunction and vascular inflammation.

Recombinant IL21 impairs endothelium-dependent relaxation ex vivo and decreases nitric oxide production from cultured human aortic endothelial cells. To determine whether IL21 has direct vascular effects independent of T and B cells, we isolated third order mesenteric arterioles from WT mice and assessed endothelium-dependent relaxation to Ach before and after 1 hour of incubation with recombinant IL21 protein (100 ng/ml) or vehicle (PBS). IL21 but not vehicle treatment resulted in impaired endothelium-dependent relaxation (**Figures 8A-B**). We have previously shown that vascular NO levels are decreased in WT mice in response to Ang II infusion (19). To determine the effect of IL21 on endothelial NO production, we cultured human aortic endothelial cells (HAECs) with vehicle or recombinant IL21 and assessed NO production using flow cytometry with the DAF-FM dye. IL21 decreased NO production from these cells (**Figure 8C**). Thus, IL21 has direct detrimental effects on the vessel wall independent of alterations in T and B cells.

$CD4^+$ T cell production of IL21 correlates with systolic BP and IL17A in humans. To determine the relevance of our findings to human hypertension, we quantified IL21 and IL17A production from cultured $CD4^+$ T cells isolated from the peripheral blood of 37 subjects (**Figure 9A and Table S1)**. Systolic BP (SBP) was measured on the day of blood draw and significantly correlated with IL21 levels (**Figure 9B**). In addition, when stratified by SBP less than or greater than or equal to 130 mmHg, IL21 production from $CD4^+$ T cells was significantly higher in those with SBP greater than or equal to 130 mmHg (**Figure 9C**). In this sample set, IL21 levels did not differ significantly between blacks and whites or males and females and did not correlate with BMI or age. Furthermore, T cell production of IL21 strongly correlated with IL17A production (**Figure 9D**), and this correlation remained significant in multivariate analysis after controlling for race, gender, age, and BMI. This finding suggests that the same or similar cells are producing IL21 and IL17A in

human hypertension and/or that one cytokine strongly regulates the other. As described above, IL21 is known to promote IL17A production. Taken together, these data suggest that IL21 and the cells that produce it are an attractive therapeutic target for hypertension and its vascular complications.

DISCUSSION

It is now evident that hypertension is an inflammatory disease with key roles played by most innate and adaptive immune cells including DCs, monocytes/macrophages, gamma delta ($\gamma\delta$) T cells, $CD4^+$ T helper cells, $CD8^+$ cytotoxic T cells, and B cells (7). Modest elevations of serum immunoglobulins have also been observed in both experimental and human hypertension (24, 25), but whether hypertension is associated with a GC reaction is not known. Here we show that genetic or pharmacological inhibition of IL21 results in blunted hypertension and reduced vascular inflammation/dysfunction. Since IL21 is produced primarily by Tfh cells whose main effector function is to promote a GC reaction, our data strongly suggest that hypertension is associated with a GC response. Indeed, we show accumulation of GC-like cells in the aorta and mesenteric lymph nodes and increased IgG1 production in hypertensive WT but not *Il21*$^{-/-}$ mice. Moreover, genetic deficiency of Tfh cells results in protection from chronic hypertension. Finally, we show that BP in a cohort of humans correlates with $CD4^+$ T cell production of IL21. This latter finding is consistent with a previous report showing that among patients with coronary artery disease, serum IL21 was upregulated in those with concomitant hypertension compared to those without (26).

IL21 is a pleiotropic cytokine with effects on innate and adaptive immune cells as well as non-immune cells (10, 27). IL21 has been shown to promote Th17 and Th1 cells and inhibit Treg cells (11, 20). We and others demonstrated that hypertension is associated with an increase in IL17A and IFNγ production, and that these cytokines play important roles by modulating renal sodium transporters, vascular fibrosis, and endothelial function (20, 28, 29). Here, we show that loss of IL21 abrogates hypertension-induced T cell production of IL17A and IFNγ. IL21 is also the most potent cytokine known to induce GC B cell proliferation and differentiation into antibody secreting plasma cells (20). In keeping with this, we found that hypertension is associated with increased

accumulation of GC-like cells in the vasculature and secondary lymphoid organs in an IL21 dependent manner. Finally, we show that IL21 has direct effects on vascular endothelial cells, altering bioavailability of nitric oxide and promoting endothelial dysfunction. Future studies are needed to determine mechanisms by which IL21 alters superoxide and NO levels and to investigate whether IL21 has direct effects on vascular smooth muscle cells and fibroblasts to increase chemokine expression and collagen synthesis. In line with this, it has been shown in inflammatory bowel disease that colonic myofibroblasts and epithelial cells respond to IL21 by secreting matrix metalloproteases and chemokines that recruit other inflammatory cells (27). These potential effects of IL21 in hypertension are not mutually exclusive, and thus we propose that IL21 may indeed function as a “master” cytokine in hypertension, orchestrating responses of T cells, B cells, and parenchymal cells (**Figure 10**).

The finding that hypertension is associated with a GC reaction has important therapeutic implications. The primary purpose of a GC reaction is to mount a specific and effective immune response in the setting of infection or vaccination. GCs are transient microanatomical sites in secondary or tertiary lymphoid organs where somatic hypermutation (to generate high affinity antibodies) and isotype class switching (e.g. IgM $\rightarrow$ IgG) occurs. After multiple rounds of affinity maturation, B cells exit GCs as memory B cells or long-lived plasma cells. B cells can also differentiate along an extrafollicular pathway and produce IgM or class-switched antibodies with a low degree of somatic mutation. Although autoimmune diseases may use either pathway, there is emerging data that a GC response is the predominant pathway at least in some autoimmune diseases (22, 30-32). Interestingly, Clement et al. recently demonstrated that experimental atherosclerosis is associated with an overactive Tfh-GC B cell axis in secondary lymphoid organs and increased development of tertiary lymphoid organs in the aorta. Moreover, these authors demonstrated the presence of Tfh cells within tertiary lymphoid organs of human atherosclerotic aneurysmal arteries (33). We found that experimental hypertension is associated with both

structured and unstructured T and B cell aggregates, increased accumulation of aortic Tfh and GC B cells, and an increased percent of lymph node GC B cells. To determine the role of Tfh cells in hypertension, we created mice with T cell specific deletion of the Tfh cell lineage determining transcription factor BCL6. Mice with T cell deletion of BCL6 had blunted accumulation of Tfh cells and GC B cells in the aorta and were unable to sustain the hypertensive response to chronic Ang II infusion, suggesting a critical role for a GC reaction in hypertension.

Of note, mice with T cell deletion of BCL6 exhibited a delayed protection from Ang II induced BP elevation and were not protected from vascular accumulation of other immune cells in contrast to *Il21*$^{-/-}$ mice. One explanation for this is that other immune cells such as NK T cells and/or Th17 cells are also important sources of IL21 in hypertension or are able to compensate in the presence of Tfh cell deficiency. Indeed, we detected an increase in splenic CD4+ T cell production of IL17A in the Tfh cell deficient mice following Ang II infusion. Another explanation is that our model did not deplete the Tfh-like "peripheral helper T cells" or Tph cells which do not express prototypic Tfh markers like CXCR5 or BCL6 but still produce factors important in B cell help like IL21. Recent studies demonstrate that these Tfh-like cells cooperate with B cells in unstructured aggregates of inflamed tissues and may be important in the local differentiation of B cells into antibody-secreting cells (34). For example, Rao and colleagues used mass cytometry to analyze T cells isolated from the joints and blood of patients with rheumatoid arthritis. They identified an expanded population of PD1^{hi}CXCR5^{-}CD4^{+} T cells which they named Tph cells, distinct from PD1^{hi}CXCR5^{+}CD4^{+} Tfh cells, and showed that these cells express IL21 and chemokine receptors such as CCR5 that direct migration to inflamed sites (16). Indeed, when we quantified PD1^{hi}CXCR5^{-}CD4^{+} T cells in our animal models, we detected an increase in Tph cells in the aorta of WT but not *Il21*$^{-/-}$ mice (**Figure 4C**). In addition, as expected, these cells were not reduced in mice with T cell deletion of BCL6 (**Figure 6E**). It is not clear to what extent Tph-B cell interactions in peripheral tissues are

similar to classic Tfh-GC B cell interactions in secondary lymphoid organs. Further studies are needed to elucidate the relative role of Tph vs Tfh cells in hypertension.

We and others have elucidated the role of various T effector and regulatory cell subsets in hypertension pathogenesis (7). Recently Chan et al. demonstrated that mice with genetic or pharmacological depletion of B cells develop blunted Ang II-induced hypertension (9). It has also been shown that DCs are activated in hypertension and present immunogenic isolevuglandin-modified peptides to T cells that promote T cell proliferation (23). A missing link has been how these various immune cells produce a coordinated and orchestrated response. Based on our results, we propose that hypertensive DCs induce naïve T cells to differentiate into Tfh cells. Tfh cells then induce a GC reaction in the aorta and secondary lymphoid organs leading to increased IgG production. IL21 production from Tfh cells, and perhaps other sources such as Tph and Th17 cells, promotes the production of pathogenic IL17A and IFNγ producing T cell subsets and may have direct effects on parenchymal cells leading to hypertension and end-organ dysfunction (**Figure 10**). Further studies are necessary to more precisely define the nature and mechanism of action of B cells and immunoglobulins in hypertension.

Our data reveal some subtle differences between *Il21*$^{-/-}$ animals and acute depletion of IL21 with neutralizing antibodies. Anti-IL21 antibody treatment appears to be more effective at reducing vascular inflammation. In addition, while endothelium-dependent relaxation to Ach is impaired at baseline in *Il21*$^{-/-}$ mice, anti-IL21 antibody treatment restores endothelial function to the levels seen in normotensive WT mice. When we assessed mesenteric arteriolar superoxide production in the IL21 deficient mice, it was elevated at baseline compared to WT animals. This may explain the baseline impairment in vascular function and suggests that IL21 may have some protective effects at early developmental stages or at low levels. Furthermore, compensatory changes may have occurred in the mice deficient in IL21 from birth. Nevertheless, these complementary

approaches for deleting IL21 demonstrate the critical role played by this cytokine in hypertension and end-organ damage and suggest that anti-IL21 treatment may be a promising therapeutic strategy for hypertension.

Phase I or II clinical trials using monoclonal anti-IL21 antibodies for lupus, rheumatoid arthritis, and Crohn's disease are either completed or in progress (10). Hypertension is highly prevalent in patients with autoimmune diseases, and thus it would be interesting to determine how this therapy affects BP and vascular dysfunction. However, the risk-to-benefit ratio of such therapeutics should be carefully considered since IL21 also has potent anti-tumor and anti-viral activities. In fact, IL21 is currently being investigated as a therapeutic agent in solid tumors and hematopoietic malignancies. Boosting IL21 levels may also be beneficial for viral infections such as Hepatitis B and C and HIV. Thus, tissue-restricted targeting of a specific cellular source of IL21, such as Tfh or Tph cells, if feasible, would be a more attractive therapeutic option.

In summary, we show that both experimental and human hypertension is associated with increased $CD4^+$ T cell production of IL21. Mice deficient in IL21 exhibit blunted hypertension and vascular end-organ dysfunction. Pharmacological inhibition of IL21 after the onset of hypertension lowers BP and reverses endothelial dysfunction and vascular inflammation. Furthermore, hypertension is associated with increased aortic Tfh and GC B cells, and Tfh cell deficiency protects from chronic Ang II-induced hypertension. To our knowledge, this is the first study implicating a GC reaction in hypertension and suggests that inhibition of IL21 or specific depletion of IL21 producing cells may be a novel therapeutic strategy for the treatment of hypertension and its micro- and macrovascular complications.

METHODS

Animals and Experimental Hypertension

Wild type C57BL/6J mice, CD4-cre transgenic mice (Tg^{CD4cre}), and $Bcl6^{flox/flox}$ mice were purchased from Jackson Laboratories. $Il21^{-/-}$ mice were generated as previously described (35). These mice were backcrossed greater than 10 generations to C57BL/6J mice. Age and gender matched mice between 10-12 weeks of age were used. Experimental hypertension was induced using the Ang II model or deoxycorticosterone acetate (DOCA)-salt treatment. Mice were anesthetized with isoflurane via nose cone or ketamine/xylazine (90-120 mg/kg + 10mg/kg; 1:1 volume) via intraperitoneal injection. For Ang II-induced hypertension, 28-day (Alzet, DURECT Corporation, model 2004) or 14-day (Alzet, DURECT Corporation, model 2002) osmotic minipumps were implanted subcutaneously containing Ang II (490 ng/kg/min) (Sigma Catalog #A2900) or vehicle (0.08 M sodium chloride + 1% acetic acid solution). For DOCA-salt treatment, uninephrectomy was performed, a DOCA pellet (100mg; Innovative Research of America) was implanted subcutaneously, and the drinking water was supplemented with 1% NaCl for 21 days. Animals were euthanized after 7, 14, 21, or 28 days as indicated by CO_2 inhalation.

Blood pressure (BP) measurement

BP was measured twice weekly and averaged using a noninvasive tailcuff platform (Hatteras) or invasively by carotid radiotelemetry as previously described (14). Mice were allowed to recover for 10-14 days post-telemetry implantation prior to obtaining baseline BPs and implantation of osmotic minipumps.

Murine T cell isolation, culture, and cytokine quantification

Spleen homogenates were filtered through a 40 μm cell strainer followed by depletion of red blood cells using red blood cell lysis buffer (eBioscience). $CD4^+$ and $CD8^+$ T cells were isolated from splenic single-cell suspensions using Miltenyi cell separation kits according to the manufacturer's instructions and sorted using an AutoMACS magnetic cell sorter (Miltenyi Biotec). Cells were

plated in RPMI 1640 media + 10% FBS+ 1% penicillin/streptomycin + 50μM β-mercaptoethanol at a density of 200,000 cells/100μl on a non-tissue culture treated 96-well plate coated with mouse anti-CD3 (2μg/ml) and mouse anti-CD28 (2μg/ml) antibodies (BD Biosciences) for 72hours. Murine IL17A, IFNγ, interleukin 10 (IL10) and IL21 were measured from cell culture supernatants by ELISA Ready-Set-Go! Kits (eBioscience).

RNA isolation and qRT-PCR

RNA was isolated from cells using an RNeasy mini kit (Qiagen) according to the manufacturer's instructions. Total RNA concentration was measured using a DS-11 spectrophotometer (DeNovix). A High-Capacity cDNA Reverse Transcription kit (Applied Biosystems) was used according to the manufacturer's instructions to make cDNA. The Taqman assay system (Thermo Fisher Scientific) was used to detect *Il21*, *Bcl6*, and *Gapdh* (endogenous control). Relative quantification was determined using the comparative CT method with data normalized to *Gapdh* and calibrated to the average of the control group.

Immunohistochemistry, histological staining, and imaging

10% formalin-fixed, paraffin-embedded tissue sections of aorta or spleen from WT or *Il21*$^{-/-}$ mice treated with 28 days of Ang II or vehicle were sectioned at 5 micron thickness. Slides were labeled with anti-CD3 (ab16669, Abcam, 1:250 dilution), anti-B220 (553086, BD Pharmingen, 1:20,000 dilution), or PNA (B1075, Vector, 1:250 dilution) to detect T cells, B cells, and GC B cells, respectively. For collagen staining, slides were stained with Masson's Trichrome Blue or Picrosirius Red as previously described (19, 36). Slides were imaged at 20x using a Leica SCN400 Slide Scanner and acquired and exported using Leica Biosystems.

Vascular reactivity studies

Isometric tension studies were conducted using 2-mm segments of third-order mesenteric arterioles dissected free of perivascular fat. Studies were performed in a small vessel horizontal

wire myograph (Danish Myo Technology, models 610M and 620M) as previously described (14). Vessels were pre-constricted with norepinephrine prior to treatment with increasing doses of acetylcholine (Ach) or sodium nitroprusside (SNP). For ex vivo IL21 treatment experiments, vessels were incubated with recombinant murine IL21 (100 ng/ml; Peprotech) or vehicle (phosphate buffered saline (PBS)) in the organ chamber for 1 hr between assessments of endothelium-dependent relaxation to Ach.

Mesenteric vessel superoxide measurement

Superoxide levels were measured from mesenteric arterioles by quantification of 2-hydroxyethidium (2-OH Eth) from dihydroethidium (DHE) by high performance liquid chromatography. The 2-OH Eth product specifically reflects the interaction of DHE with superoxide as previously validated (37).

Fluorescent flow cytometry staining of lymph node and aortic leukocytes

Mesenteric lymph nodes free of surrounding fat were homogenized and filtered through a 40 μm cell strainer. Single-cell suspensions of whole aorta with adjacent perivascular fat were isolated as previously described (38). Samples were stained for viability and surface markers using the following reagents for the *T cell panel*: LIVE/DEAD Fixable Violet Dead Cell Stain (Life Technologies), brilliant violet 510 (BV510) anti-CD45 (Biolegend, clone 30-F11), peridinin chlorophyll protein-cyanin-5.5 (PerCp-Cy5.5) anti-CD3 antibody (BioLegend, clone 17A2), allophycocyanin (APC) anti-CD8 antibody (eBioscience, clone 53-6.7), allophycocyanin-cyanin-7 (APC-Cy7) anti-CD4 antibody (Biolegend, clone GK1.5), phycoerythrin-cyanin-7 (PE-Cy7) anti-CXCR5 antibody (BD Pharmingen, clone 2G8), and fluorescein isothiocyanate (FITC) anti-PD1 (eBioscience, clone J43); *B cell panel*: LIVE/DEAD Fixable Violet Dead Cell Stain (Life Technologies), BV510 anti-CD45 (Biolegend, clone 30-F11), PerCp-Cy5.5 anti-CD45R/B220 antibody (BD Biosciences, clone RA3-6B2), APC anti-IgD antibody (eBioscience, clone 11-26), APC-Cy7 anti-CD138 antibody (Biolegend, clone 281-2), PE-Cy7 anti-CD19 antibody (BD

Pharmingen, clone 1D3), phycoerythrin (PE) anti- GL7 (Invitrogen, clone GL-7), FITC anti-Fas (eBioscience, clone 15A7); *Innate immune cell panel*: LIVE/DEAD Fixable Violet Dead Cell Stain (Life Technologies), BV510 anti-CD11b (Biolegend, clone M1/70), PerCp-Cy5.5 anti-CD3 antibody (BioLegend, clone 17A2), APC anti-NK1.1 antibody (Biolegend, clone PK136), APC-Cy7 anti-F4/80 antibody (Biolegend, clone BM8), PE anti-Ly6G (Biolegend, clone 1A8) and FITC anti-CD45 (Biolegend, clone 30-F11). Staining was performed in 100μl. All antibodies were used at 1:100 dilution. Samples were acquired on a BD FACSCanto II system and analyzed using CytoBank. Gates were applied using fluorescence minus one (FMO) controls. A known quantity of counting beads (123count eBeads, eBioscience) were added to each sample prior to acquisition. Results were normalized using the bead count.

Antibody treatments

Mice were implanted with 28-day osmotic minipumps containing Ang II. After 14 days of Ang II infusion, mice were randomized to either an isotype control group (eBioscience, rat IgG2 k isotype control functional grade purified, clone eBRa) or mouse anti-IL21 treatment group (eBioscience, anti-mouse anti-IL21 functional grade purified, clone FFA21). Treatment was administered by intraperitoneal injection with 100μg of antibody twice a week for the last 2 weeks of Ang II infusion (days 16, 19, 22, and 25). This regimen was chosen based on prior studies (39).

Plasma immunoglobulin isolation and quantification

Mice were euthanized, and whole blood was collected by direct cardiac puncture into an EDTA coated syringe. Blood was immediately centrifuged, and plasma stored at -80°C. Plasma immunoglobulin was quantified using LEGENDplex Mouse Immunoglobulin Isotyping Panel (Biolegend) according to the manufacturer's instructions.

Dendritic cell (DC)-CD4$^+$ T cell co-culture

Splenic single cell suspensions were generated as described above. Dendritic cells ($CD11c^+$) and naïve $CD4^+$ T cells ($CD44^-$) were enriched using Miltenyi cell separation kits (Cat no 130-108-338 and 130-104-453) according to the manufacturer's instructions and sorted using an AutoMACS magnetic cell sorter (Miltenyi Biotec). 200,000 cells were plated in duplicate at a 1:5 ratio (DC:T) in RPMI 1640 media + 10% FBS+ 1% penicillin/streptomycin + 50μM β-mercaptoethanol + 1mM Sodium Pyruvate + 1% L-glutamine at a density of $1x10^6$ cells/ml in a tissue culture treated 96-well round bottom plate for 72 hours.

Nitric oxide measurement from cultured endothelial cells

Human aortic endothelial cells were purchased from Lonza (CC-2535; Lot No. 0000297640) and grown to 90% confluency in endothelial cell growth medium (PromoCell). The cells were detached using trypsin, resuspended in endothelial cell media, and allowed to rest for 30 minutes at 37 degrees. Cells were loaded for 30 minutes with 1μM of 4-Amino-5-Methylamino-2',7'-Difluorofluorescein Diacetate (DAF-FM diacetate; ThermoFisher) dissolved in DMSO. Cells were then incubated with 100 ng/mL of recombinant human interleukin-21 (PeproTech) or vehicle (PBS). After 15 minutes, the cells were acquired via flow cytometry. Gating and data analysis were performed in FlowJo.

Human Subjects

Blood samples were obtained as part of Vanderbilt's American Heart Association Strategically Focused Research Network protocol. Inclusion criteria were age 30-80 years, systolic blood pressures 110-150 mmHg and/or diastolic blood pressure 80-99 mmHg on the day of the study visit. Blood pressure (BP) was measured in the seated position after a 10-15 min rest period by an automated cuff (GE CRITIKON Dinamap Pro 1000). Exclusion criteria were pregnancy, intolerance to study protocols, acute cardiovascular events within the previous 6 months, impaired renal function (estimated GFR < 45 ml/min/1.73m^2), current or recent (within 1 month) treatment with systemic glucocorticoid therapy, current use of hypertensive drugs (except calcium channel

blockers and beta blockers), pharmacologically treated diabetes mellitus, morbid obesity (BMI >45), prior adverse reaction to thiazide or spironolactone, contraindications to MRI, impaired hepatic function (aspartate amino transaminase and/or alanine amino transaminase > 1.5x upper limit of normal range), current illicit drug use, and sexually active women of childbearing potential not conforming to use of birth control.

Human T cell isolation, culture, and cytokine quantification

Peripheral blood mononuclear cells (PBMCs) were isolated from whole blood by Ficoll plaque centrifugation (GE Life Science). $CD4^+$ T cells were isolated from the Ficoll buffy coat using Miltenyi cell separation kits according to the manufacturer's instructions and sorted using an AutoMACS magnetic cell sorter (Miltenyi Biotec). Cells were plated in RPMI 1640 media + 10% FBS+ 1% penicillin/streptomycin + 50μM β-mercaptoethanol at a density of 200,000 cells/200μl on a non-tissue culture treated 96-well plate coated with human anti-CD3 (2μg/ml) and human anti-CD28 (2μg/ml) antibodies (BD Biosciences) for 72 hours. Human IL21 and IL17A was measured from cell culture supernatants by LEGENDplex bead assay (Biolegend).

Statistics

All data are expressed as mean ± SEM or as box and whisker plots as indicated. Data were analyzed in GraphPad Prism or R using Student's *t*-test (for 2 group comparisons) or 2-way ANOVA (for multiple group comparisons). Nonparametric 2 group data were analyzed by Mann Whitney test. Vascular relaxation studies were compared using area under the curve analysis. Human cytokine data were log transformed for Pearson's correlation analysis. $P < 0.05$ was considered significant.

Study approvals

All animal procedures were approved by the Vanderbilt IACUC. The human studies were approved by the Vanderbilt Institutional Review Board (IRB#141382) and conforms to the

standards set forth by the US Federal Policy for the Protection of Human Subjects. All human subjects provided written informed consent prior to inclusion in the study.

AUTHOR CONTRIBUTIONS

BLD and MSM designed the experiments. BLD, AKP, YC, CDS, FL, MA, LX, HAI, AED, SID, AEN, HMSA, and MRA generated data. BLD, AKP, MA, AED, SZ, and MSM analyzed data. MSM supervised the study.

JDF, NRB, JPV, SMD, AA generated human data. BLD, FE, and MSM analyzed human data. TAI and MSM supervised the human study.

BD, AKP, FL, NRB, FE, JPV and MSM wrote the manuscript and revised it for intellectual content.

ACKNOWLEDGEMENTS

We acknowledge the Vanderbilt Translational Pathology Shared Resource (NIH Cancer Center 5P30 CA68485-19), Digital Histology Shared Resource at Vanderbilt University Medical Center (www.mc.vanderbilt.edu/dhsr), and the Vanderbilt Free Radicals in Medicine Core (FRIMCORE) (NIH P01 HL129941). This work was supported by an NIH T32 training grant (T32 HL069765-11A1) and an American Heart Association (AHA) predoctoral fellowship award (17PRE33460032) to BLD; an NIH T32 training grant (T32 HL7411-37) to AKP; an AHA Strategically Focused Prevention Research Network award to AI and MSM; a Veterans Affairs Merit Review award (IBX000915A) and a pilot grant through Vanderbilt University Medical Center's Digestive Disease Research Center supported by NIH grant P30DK058404 (to HMSA); an NIH K08 award (HL121671) and an NIH DP2 award (HL137166) to MSM. The authors declare no competing financial interests.

REFERENCES

1. Whelton PK, Carey RM, Aronow WS, Casey DE, Jr., Collins KJ, Dennison Himmelfarb C, et al. 2017 ACC/AHA/AAPA/ABC/ACPM/AGS/APhA/ASH/ASPC/NMA/PCNA Guideline for the Prevention, Detection, Evaluation, and Management of High Blood Pressure in Adults: A Report of the American College of Cardiology/American Heart Association Task Force on Clinical Practice Guidelines. *Hypertension.* 2017.
2. Collaborators GBDRF. Global, regional, and national comparative risk assessment of 79 behavioural, environmental and occupational, and metabolic risks or clusters of risks, 1990-2015: a systematic analysis for the Global Burden of Disease Study 2015. *Lancet.* 2016;388(10053):1659-724.
3. Nwankwo T, Yoon SS, Burt V, and Gu Q. Hypertension Among Adults in the United States: National Health and Nutrition Examination Survey, 2011-2012. http://www.cdc.gov/nchs/data/databriefs/db133.pdf.
4. Okuda T, and Grollman A. Passive transfer of autoimmune induced hypertension in the rat by lymph node cells. *Tex Rep Biol Med.* 1967;25(2):257-64.
5. White FN, and Grollman A. Autoimmune Factors Associated with Infarction of the Kidney. *Nephron.* 1964;1:93-102.
6. Guzik TJ, Hoch NE, Brown KA, McCann LA, Rahman A, Dikalov S, et al. Role of the T cell in the genesis of angiotensin II induced hypertension and vascular dysfunction. *J Exp Med.* 2007;204(10):2449-60.
7. Norlander AE, Madhur MS, and Harrison DG. The immunology of hypertension. *J Exp Med.* 2018;215(1):21-33.
8. Norlander AE, and Madhur MS. Inflammatory Cytokines Regulate Renal Sodium Transporters: How, Where, and Why? *Am J Physiol Renal Physiol.* 2017:ajprenal 00465 2016.

9. Chan CT, Sobey CG, Lieu M, Ferens D, Kett MM, Diep H, et al. Obligatory Role for B Cells in the Development of Angiotensin II-Dependent Hypertension. *Hypertension.* 2015;66(5):1023-33.

10. Spolski R, and Leonard WJ. Interleukin-21: a double-edged sword with therapeutic potential. *Nat Rev Drug Discov.* 2014;13(5):379-95.

11. Carbo A, Olivares-Villagomez D, Hontecillas R, Bassaganya-Riera J, Chaturvedi R, Piazuelo MB, et al. Systems modeling of the role of interleukin-21 in the maintenance of effector CD4+ T cell responses during chronic Helicobacter pylori infection. *MBio.* 2014;5(4):e01243-14.

12. Linterman MA, Beaton L, Yu D, Ramiscal RR, Srivastava M, Hogan JJ, et al. IL-21 acts directly on B cells to regulate Bcl-6 expression and germinal center responses. *J Exp Med.* 2010;207(2):353-63.

13. Ozaki K, Spolski R, Feng CG, Qi CF, Cheng J, Sher A, et al. A critical role for IL-21 in regulating immunoglobulin production. *Science.* 2002;298(5598):1630-4.

14. Norlander AE, Saleh MA, Pandey AK, Itani HA, Wu J, Xiao L, et al. A salt-sensing kinase in T lymphocytes, SGK1, drives hypertension and hypertensive end-organ damage. *JCI insight.* 2017;2(13):e92801.

15. Magliozzi R, Howell O, Vora A, Serafini B, Nicholas R, Puopolo M, et al. Meningeal B-cell follicles in secondary progressive multiple sclerosis associate with early onset of disease and severe cortical pathology. *Brain.* 2007;130(Pt 4):1089-104.

16. Rao DA, Gurish MF, Marshall JL, Slowikowski K, Fonseka CY, Liu Y, et al. Pathologically expanded peripheral T helper cell subset drives B cells in rheumatoid arthritis. *Nature.* 2017;542(7639):110-4.

17. Chang A, Henderson SG, Brandt D, Liu N, Guttikonda R, Hsieh C, et al. In situ B cell-mediated immune responses and tubulointerstitial inflammation in human lupus nephritis. *J Immunol.* 2011;186(3):1849-60.

18. Madhur MS, Lob HE, McCann LA, Iwakura Y, Blinder Y, Guzik TJ, et al. Interleukin 17 promotes angiotensin II-induced hypertension and vascular dysfunction. *Hypertension.* 2010;55(2):500-7.

19. Saleh MA, McMaster WG, Wu J, Norlander AE, Funt SA, Thabet SR, et al. Lymphocyte adaptor protein LNK deficiency exacerbates hypertension and end-organ inflammation. *J Clin Invest.* 2015;125(3):1189-202.

20. Lei L, Zhong XN, He ZY, Zhao C, and Sun XJ. IL-21 induction of CD4+ T cell differentiation into Th17 cells contributes to bleomycin-induced fibrosis in mice. *Cell Biol Int.* 2015;39(4):388-99.

21. Mesin L, Ersching J, and Victora GD. Germinal Center B Cell Dynamics. *Immunity.* 2016;45(3):471-82.

22. DeFranco AL. Germinal centers and autoimmune disease in humans and mice. *Immunol Cell Biol.* 2016;94(10):918-24.

23. Kirabo A, Fontana V, de Faria AP, Loperena R, Galindo CL, Wu J, et al. DC isoketal-modified proteins activate T cells and promote hypertension. *J Clin Invest.* 2014;124(10):4642-56.

24. Chan CT, Lieu M, Toh BH, Kyaw TS, Bobik A, Sobey CG, et al. Antibodies in the pathogenesis of hypertension. *Biomed Res Int.* 2014;2014:504045.

25. Wang X, Li Y, Li H, Gu Y, Song Y, Zhang Q, et al. Relationship of serum immunoglobulin levels to blood pressure and hypertension in an adult population. *J Hum Hypertens.* 2018;32(3):212-8.

26. Ding R, Gao W, He Z, Liao M, Wu F, Zou S, et al. Effect of serum interleukin 21 on the development of coronary artery disease. *APMIS.* 2014;122(9):842-7.

27. Liu SM, and King C. IL-21-producing Th cells in immunity and autoimmunity. *J Immunol.* 2013;191(7):3501-6.

28. Norlander AE, Saleh MA, Kamat NV, Ko B, Gnecco J, Zhu L, et al. Interleukin-17A Regulates Renal Sodium Transporters and Renal Injury in Angiotensin II-Induced Hypertension. *Hypertension.* 2016;68(1):167-74.

29. Wu J, Saleh MA, Kirabo A, Itani HA, Montaniel KR, Xiao L, et al. Immune activation caused by vascular oxidation promotes fibrosis and hypertension. *J Clin Invest.* 2016;126(1):50-67.

30. Pissani F, and Streeck H. Emerging concepts on T follicular helper cell dynamics in HIV infection. *Trends Immunol.* 2014;35(6):278-86.

31. Nutt SL, Hodgkin PD, Tarlinton DM, and Corcoran LM. The generation of antibody-secreting plasma cells. *Nat Rev Immunol.* 2015;15(3):160-71.

32. De Silva NS, and Klein U. Dynamics of B cells in germinal centres. *Nat Rev Immunol.* 2015;15(3):137-48.

33. Clement M, Guedj K, Andreata F, Morvan M, Bey L, Khallou-Laschet J, et al. Control of the T follicular helper-germinal center B-cell axis by CD8(+) regulatory T cells limits atherosclerosis and tertiary lymphoid organ development. *Circulation.* 2015;131(6):560-70.

34. Hutloff A. T Follicular Helper-Like Cells in Inflamed Non-Lymphoid Tissues. *Frontiers in immunology.* 2018;9:1707.

35. Yi JS, Du M, and Zajac AJ. A vital role for interleukin-21 in the control of a chronic viral infection. *Science.* 2009;324(5934):1572-6.

36. Laroumanie F, Korneva A, Bersi MR, Alexander MR, Xiao L, Zhong X, et al. LNK deficiency promotes acute aortic dissection and rupture. *JCI insight.* 2018;3(20).

37. Fink B, Laude K, McCann L, Doughan A, Harrison DG, and Dikalov S. Detection of intracellular superoxide formation in endothelial cells and intact tissues using dihydroethidium and an HPLC-based assay. *Am J Physiol Cell Physiol.* 2004;287(4):C895-902.

38. Laroumanie F, Dale BL, Saleh MA, and Madhur MS. Intracellular Staining and Flow Cytometry to Identify Lymphocyte Subsets Within Murine Aorta, Kidney and Lymph Nodes in a Model of Hypertension. *Journal of Visualized Experiments.* 2017;119:e55266.

39. Saleh MA, Norlander AE, and Madhur MS. Inhibition of Interleukin-17A, But Not Interleukin-17F, Signaling Lowers Blood Pressure, and Reduces End-Organ Inflammation in Angiotensin II–Induced Hypertension. *JACC: Basic to Translational Science.* 2016;1(7):606-16.

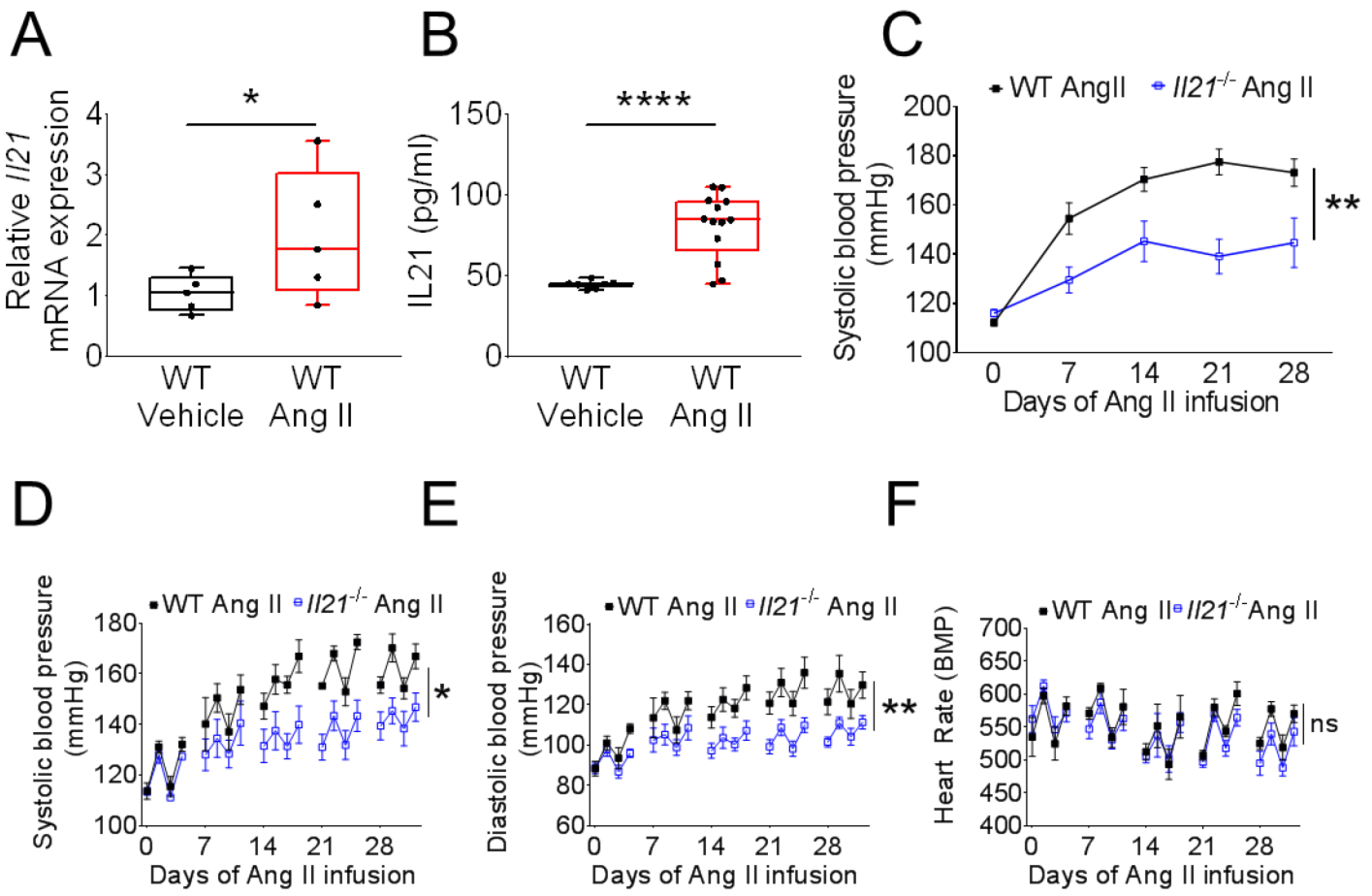

Figure 1. Hypertension is associated with increased CD4⁺ T cell production of interleukin 21 (IL21), and IL21 deficiency blunts the hypertensive response to Ang II infusion. (**A**) Relative *Il21* mRNA expression by quantitative real time PCR from splenic CD4+ T cells cultured for 72 hours with anti-CD3/anti-CD28 coated plates (n=5). (**B**) IL21 protein was quantified in culture supernatants by ELISA (n=7-13). (**C**) Systolic blood pressure was measured by tail-cuff weekly over 28 days of Ang II infusion in wild type (WT) and *Il21*$^{-/-}$ mice (n=8-9). (**D**) Systolic blood pressure, (**E**) diastolic blood pressure, and (**F**) heart rate were measured invasively weekly using carotid radiotelemetry over 28 days of Ang II infusion in WT and *Il21*$^{-/-}$ mice (n=5-8). Data are expressed as box and whisker plots (**A-B**) or mean ± SEM (C-F); *P<0.05, **P<0.01, ****P<0.0001 by Student's t-test (**A-B**) or 2-way ANOVA with repeated measures (**C-F**).

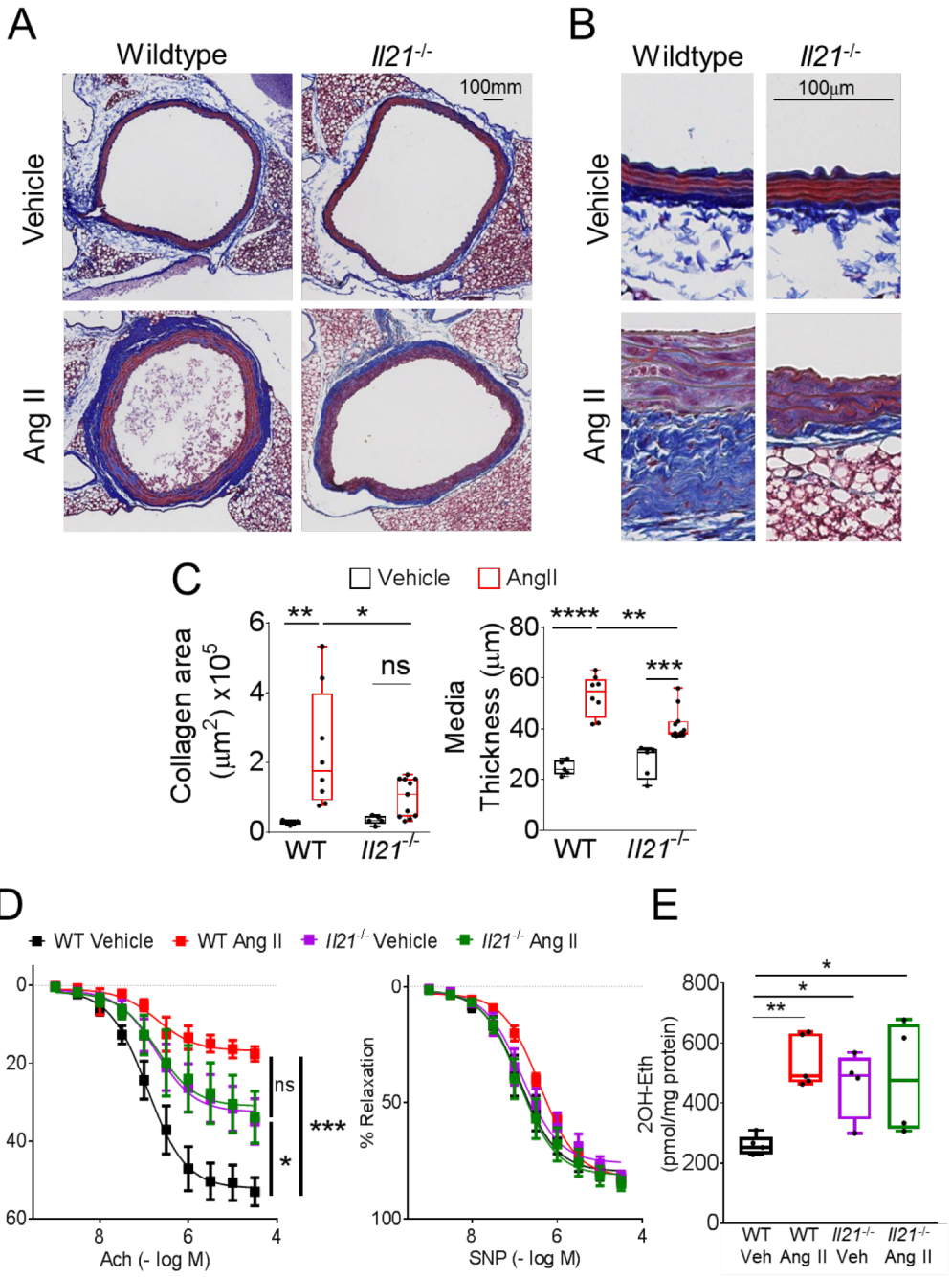

Figure 2. Loss of IL21 protects against Ang II-induced vascular remodeling and endothelial dysfunction. WT and *Il21*$^{-/-}$ mice were infused with Ang II or vehicle for 28 days. Representative images of (**A**) bright field aortic collagen deposition and (**B**) media thickness by Masson's trichrome blue staining. (**C**) Quantification of aortic collagen deposition area and media thickness (n=5-11). (**D**) Endothelium-dependent relaxation in response to increasing doses of acetylcholine (Ach) (left) and endothelium-independent relaxation in response to increasing doses of sodium nitroprusside (SNP) (right) were measured in isolated mesenteric arterioles (n=6-8). (**E**) Superoxide levels from mesenteric arterioles as measured by quantification of 2-hydroxyethidium (2OH-Eth) (n=4-5). Data are expressed as box and whisker plots (**C and E**) or mean ± SEM (**D**); **P*<0.05, ***P*<0.01, ****P*<0.001, *****P*<0.0001 by 2-way ANOVA (**C-E**).

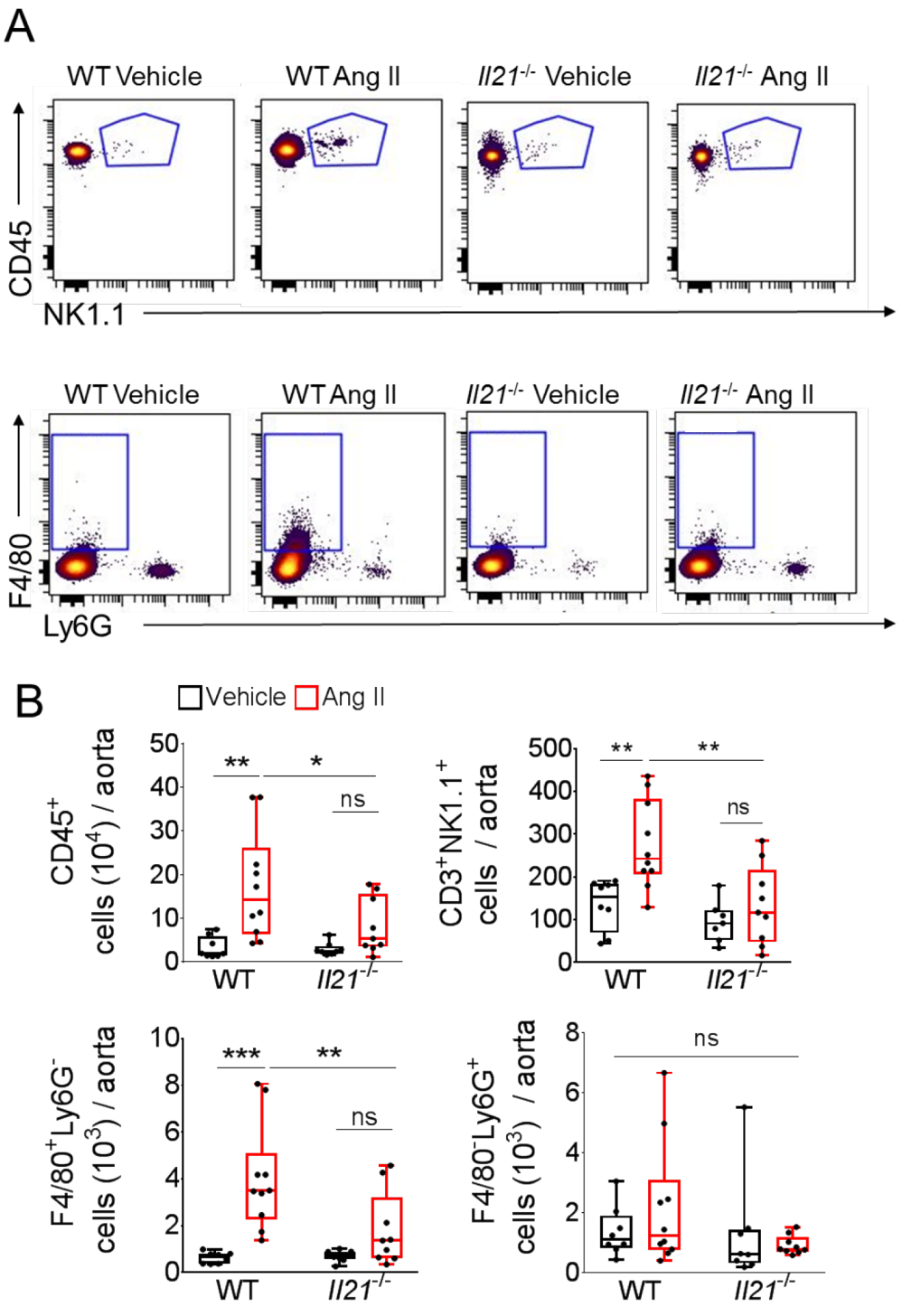

Figure 3. IL21 deficiency blunts early vascular infiltration of natural killer (NK) T cells and macrophages. (**A**) Representative flow cytometry bi-axial plots for NK T cells (NK1.1$^+$), macrophages (F4/80$^+$Ly6G$^-$), and neutrophils (F4/80$^-$Ly6G$^+$) in the aorta of WT and *Il21*$^{-/-}$ mice infused with Ang II or vehicle for 7 days. (**B**) Summary quantification of leukocytes (CD45$^+$ cells), NK T cells (CD3$^+$NK1.1$^+$ cells), macrophages (F4/80$^+$Ly6G$^-$), and neutrophils (F4/80$^-$Ly6G$^+$) (n=7-10). Data are expressed as box and whisker plots; **P*<0.05, ***P*<0.01, ****P*<0.001 by 2-way ANOVA.

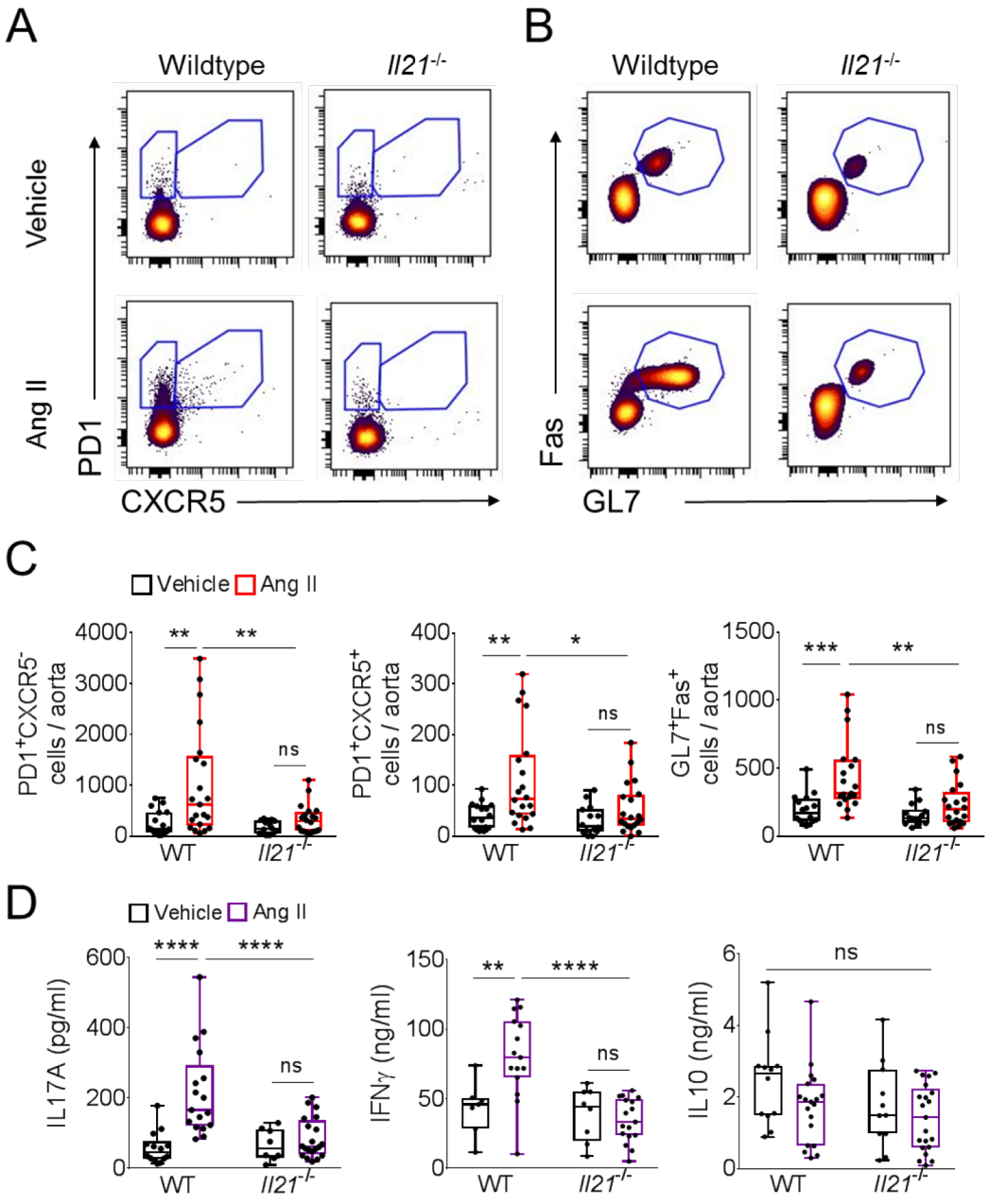

Figure 4. Hypertension induces peripheral T helper (Tph), T follicular helper (Tfh), and germinal center (GC) B cells in the aorta in an IL21 dependent manner. (**A**) Representative flow cytometry bi-axial plots for Tph ($PD1^+CXCR5^-$), Tfh ($PD1^+CXCR5^+$) cells, and (**B**) GC B cells ($GL7^+Fas^+$) in the aorta of WT and *Il21*$^{-/-}$ mice infused with Ang II or vehicle for 28 days. (**C**) Summary quantification of Tph, Tfh, and GC B cells (n=14-20). (**D**) Splenic $CD4^+$ T cell production of interleukin 17A (IL17A) and interleukin 10 (IL10) and $CD8^+$ T cell production of interferon gamma (IFNγ) from WT and *Il21*$^{-/-}$ mice infused with Ang II or vehicle for 28 days quantified by ELISA (n=7-21). Data are expressed as box and whisker plots; **P*<0.05, ***P*<0.01, ****P*<0.001, *****P*<0.0001 by 2-way ANOVA.

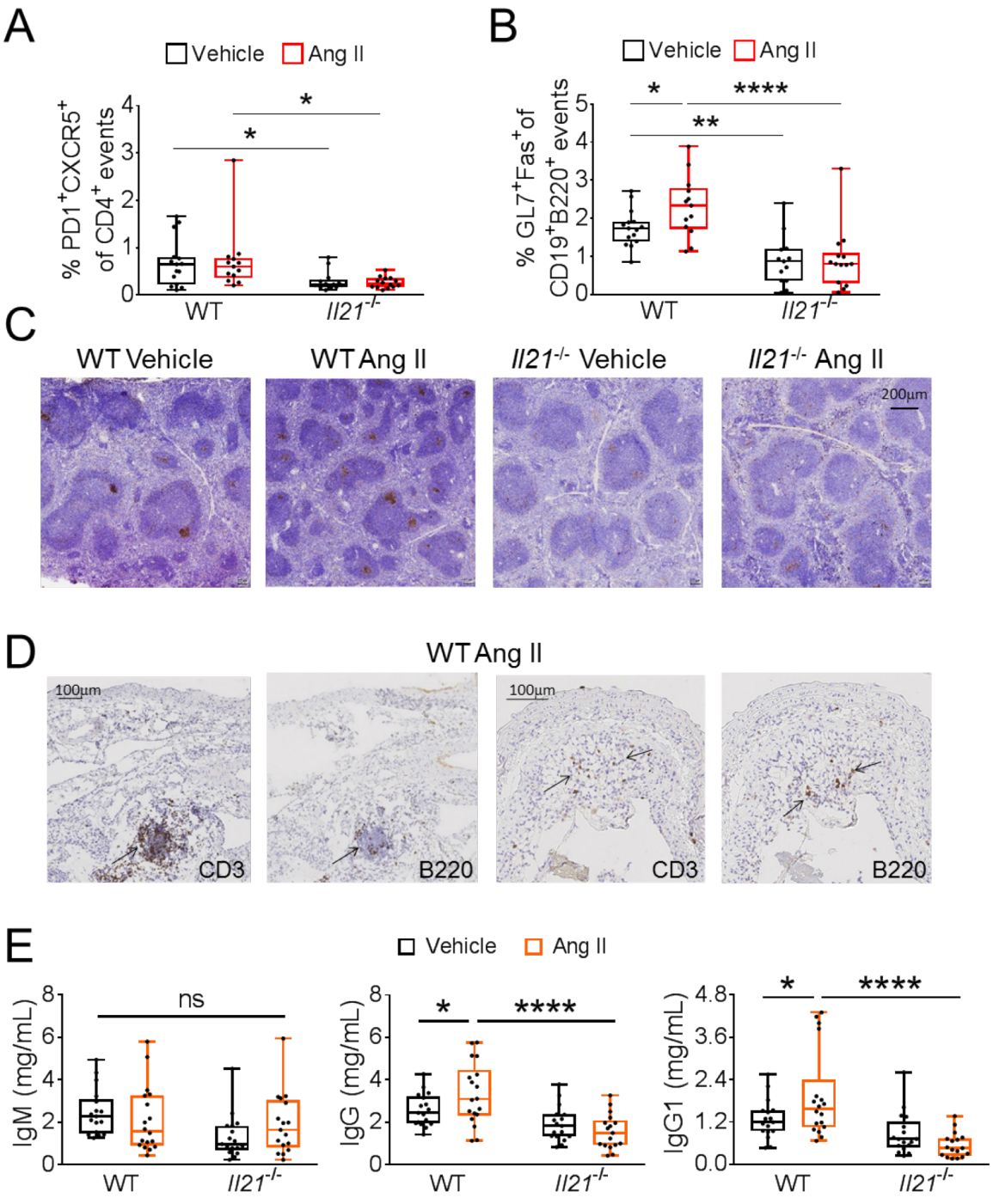

Figure 5. Hypertension induces an IL21 dependent germinal center (GC) response, tertiary lymphoid development, and increased IgG production. WT and *Il21*$^{-/-}$ mice were infused with Ang II or vehicle for 28 days. (**A**) Percent Tfh cells (PD1^{+}CXCR5^{+}) of CD4^{+} T cells and (**B**) percent GC B cells (GL7^{+}Fas^{+}) of total CD19^{+}B220^{+} B cells from mesenteric lymph nodes (n=13-15). (**C**) Bright field images of splenic cross sections stained for the GC B cell marker PNA (representative of n=4-7). (**D**) Example bright field images of aortic sections stained for CD3 (T cells) and B220 (B cells). (**E**) Plasma immunoglobulin concentration of IgM, IgG, and IgG1 (n=17-18). Data are expressed as box and whisker plots; *P<0.05, **P<0.01, ****P<0.0001 by 2-way ANOVA.

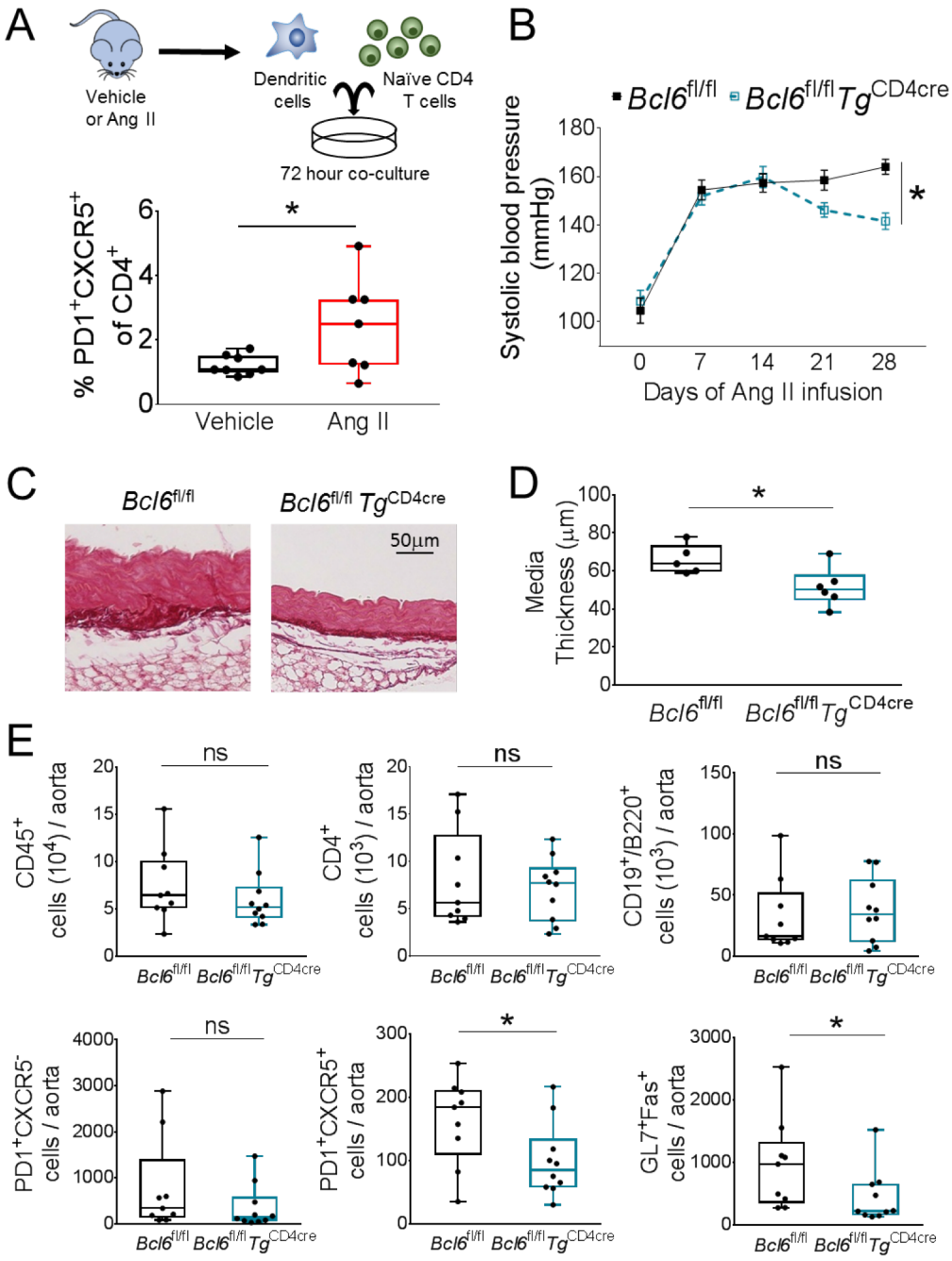

Figure 6. Hypertensive DCs induce Tfh cell polarization, and Tfh cells play a critical role in hypertension. (**A**) DCs were isolated from the spleen of WT mice infused with Ang II or vehicle for 14 days and co-cultured with splenic naïve CD4⁺ T cells from vehicle infused WT mice (top). Percent Tfh cells (PD1⁺CXCR5⁺) of CD4⁺ T cells was determined by flow cytometry (n=7-8) (bottom). (**B**) Systolic blood pressure was measured by tail-cuff weekly over 28 days of Ang II infusion in *Bcl6*$^{fl/fl}$*Tg*^{CD4cre} and control *Bcl6*$^{fl/fl}$ littermates (n=9-11). (**C**) Representative images of bright field aortic wall thickness by Picrosirius Red staining. (**D**) Quantification of aortic wall thickness (n=5-6). (**E**) Summary quantification of total leukocytes (CD45⁺), T helper (CD4⁺), B (CD19⁺B220⁺), Tph (PD1⁺CXCR5⁻), Tfh (PD1⁺CXCR5⁺), and GC B (GL7⁺Fas⁺) cells in the aorta from *Bcl6*$^{fl/fl}$*Tg*^{CD4cre} and control *Bcl6*$^{fl/fl}$ littermates infused with Ang II for 28 days (n=9-10). Data are expressed as box and whisker plots (**A, D-E**) or mean ± SEM (**B**); **P*<0.05 by Student's *t*-test (**A, D-E**) or 2-way ANOVA with repeated measures (**B**).

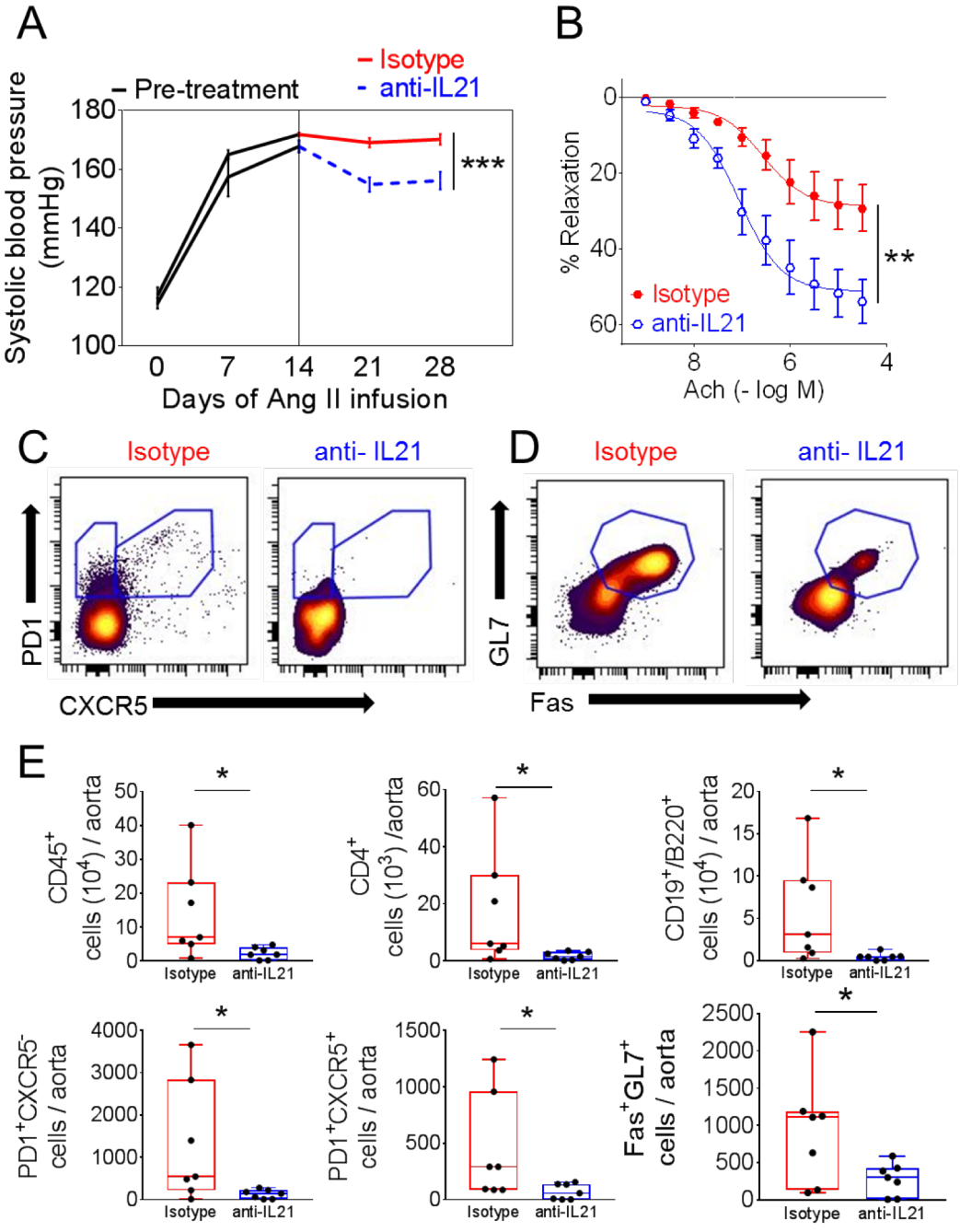

Figure 7. Anti-IL21 treatment lowers blood pressure and reverses endothelial dysfunction and vascular inflammation. (**A**) Systolic blood pressure was measured by tail-cuff weekly over 28 days of Ang II infusion. Isotype control or IL21 neutralizing antibodies were administered twice weekly during the last 2 weeks of Ang II infusion (n=7-8). (**B**) Endothelium-dependent relaxation in response to increasing doses of Ach was measured in both groups (n=7-8). (**C**) Representative flow cytometry bi-axial plots for Tph ($PD1^+CXCR5^-$), Tfh ($PD1^+CXCR5^+$), and (**D**) GC B ($GL7^+Fas^+$) cells in the aorta from both groups. (**E**) Summary quantification of total leukocytes ($CD45^+$), T helper ($CD4^+$), B ($CD19^+B220^+$), Tph, Tfh, and GC B cells from both groups (n=7). Data are expressed as mean ± SEM (**A**-**B**) or box and whisker plots (**E**); **P*<0.05, ***P*<0.01, ****P*<0.001 by 2-way ANOVA with repeated measures (**A**) or Student's *t*-test (**B, E**).

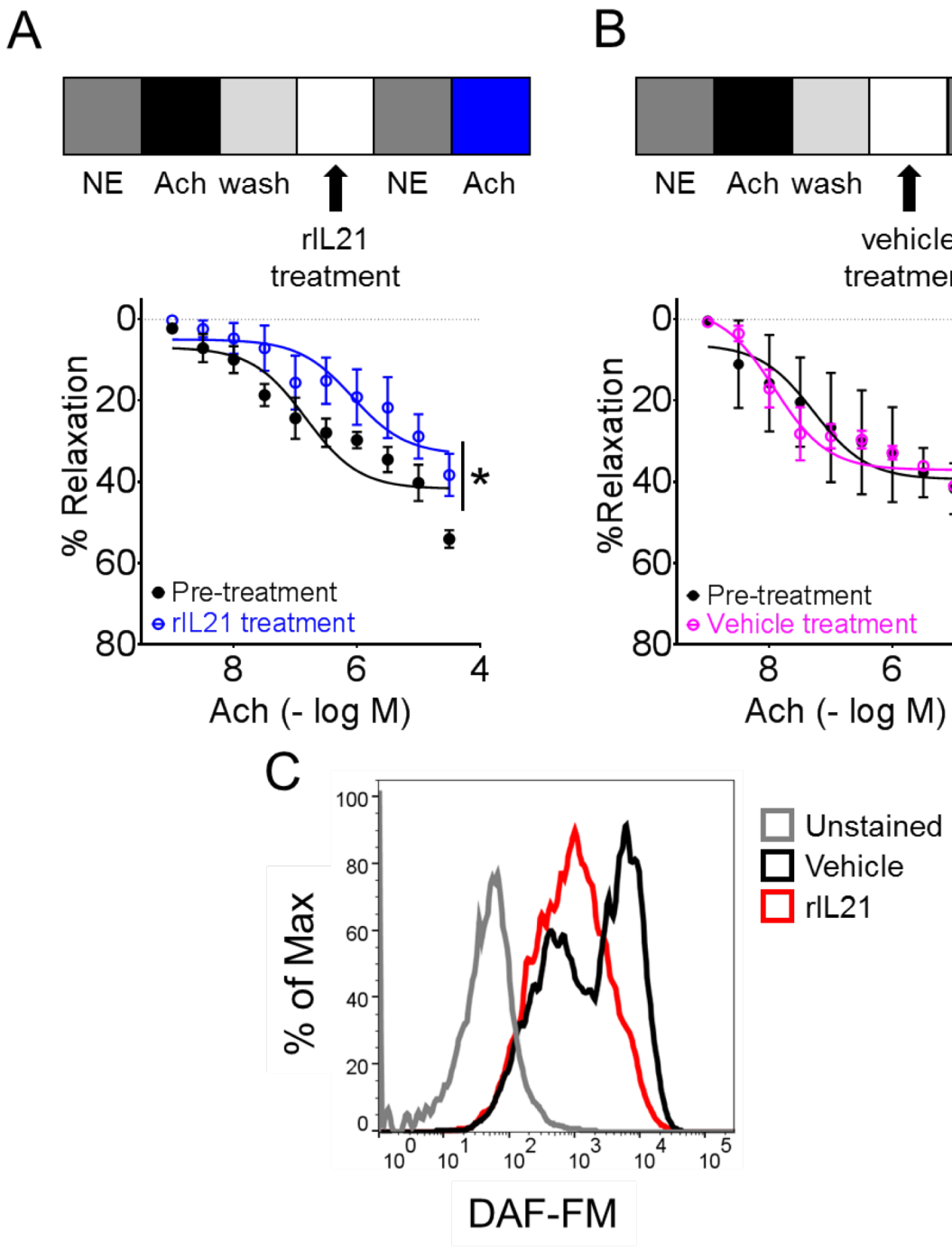

Figure 8. Recombinant IL21 impairs endothelium-dependent relaxation ex vivo and decreases nitric oxide production from cultured human aortic endothelial cells. (**A-B**) Schematic of ex vivo treatment of WT mesenteric arterioles (top) and endothelium-dependent relaxation in response to increasing doses of acetylcholine (Ach) before and after treatment with recombinant IL21 (**A**, n=5) or vehicle (**B**, n=3). NE=norepinephrine. (**C**) Histogram of 4-Amino-5-Methylamino-2',7'-Difluorofluorescein Diacetate (DAF-FM) fluorescence in cultured human aortic endothelial cells treated with recombinant IL21 or vehicle (representative of n=4). Data are expressed as mean ± SEM (**A-B**); **P*<0.05 by paired Student's *t*-test (**A-B**).

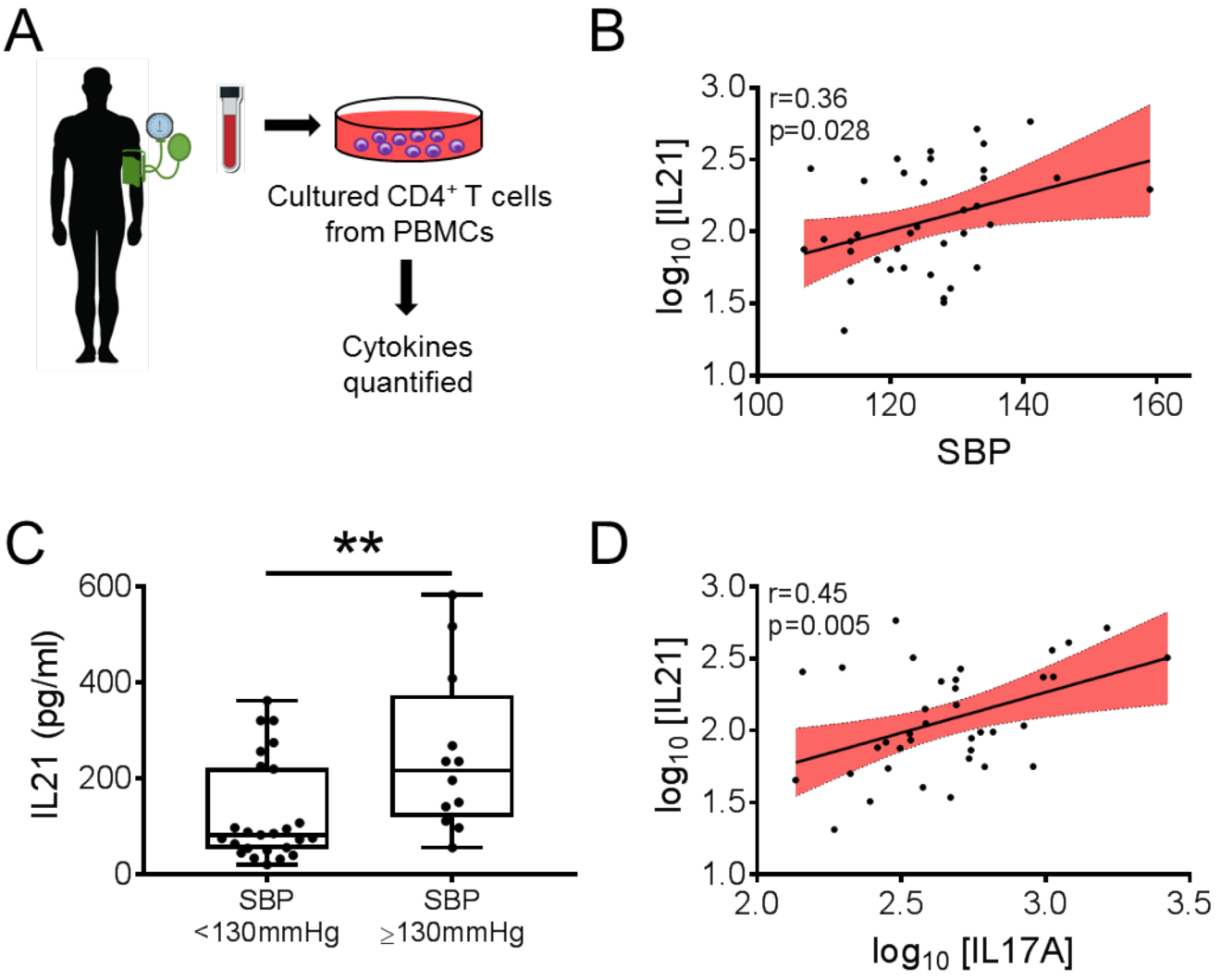

Figure 9. CD4⁺ T cell production of IL21 correlates with systolic blood pressure (SBP) and IL17A in humans. (**A**) SBP was determined at the time of blood draw in human subjects. CD4+ T cells were isolated from peripheral blood mononuclear cells (PBMCs) and cultured for 3 days. Cytokines were then quantified from the supernatants. (**B**) CD4⁺ T cell production of IL21 vs. systolic blood pressure in humans (n=37). (**C**) Human CD4⁺ T cell production of IL21 dichotomized by systolic blood pressure (SBP) <130 mmHg or ≥ 130 mmHg (n=12-25). (**D**) CD4⁺ T cell production of IL21 vs. IL17A in humans (n=37). Pearson's correlation co-efficient and corresponding p-value are shown on the graph (**B and D**). Data are expressed as box and whisker plots (**C**); ***P*<0.01 by Student's *t*-test (**C**).

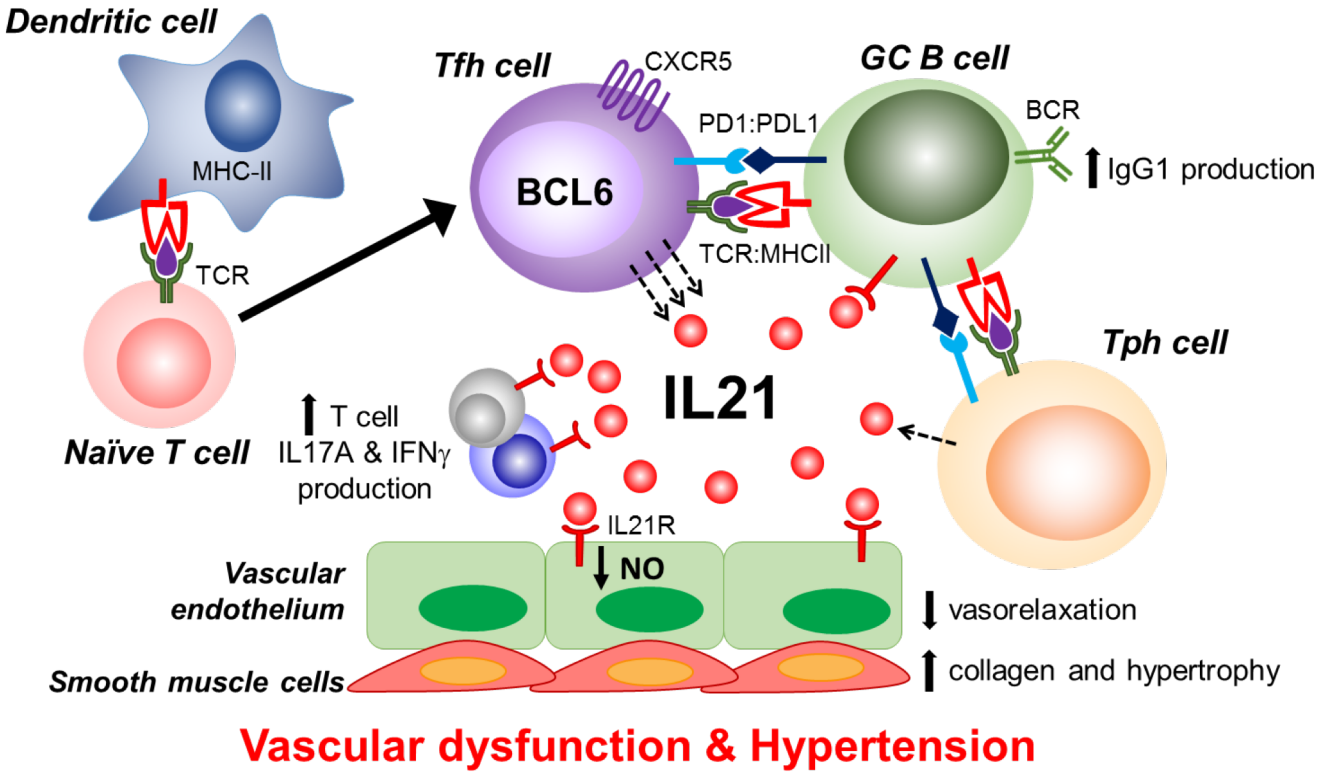

Figure 10. Working model of how IL21 functions as a master cytokine in hypertension coordinating T, B, and somatic cell responses. TCR = T cell receptor; MHCII = major histocompatibility complex II; BCR = B cell receptor; NO = nitric oxide.